24th INTERNATIONAL CONGRESS ON SOUND AND VIBRATION
23–27 July 2017, London

THE THERMAL PROTECTION AND TEST VERIFICATION FOR HYPERSONIC FLIGHT VEHICLES BY FILM COOLING

Xiang Shuhong, Zhang Minjie, Yang Yanjing, Wang Yuchen, Li Ye, Zhang Jungang, Yan tingfei and Wang Jing

Beijing Institute of Spacecraft Environment Engineering, China
email: xshxsh638@sohu.com

Xiang Shuhong

National Key Laboratory of Science and Technology on Reliability and Environment Engineering, China

Abstract: The idea of active thermal protection for hypersonic vehicles was presented. The film cooling protection of Mach 15 flow is conducted on a new cone with several designed shaped micro holes built around the stagnation point to inject coolant flow.The heat flux on the wall with film cooling at the vicinity of the hole could be reduced by almost 90% compared to that without film cooling. Tests verification through heat source of plasma and welding gun were designed to verify the effectiveness of film cooling active thermal protection, and both tests had confirmed the feasibility of this method. The study of theory calculation and tests showed promising performance of film cooling for future hypersonic vehicles.
Keywords: hypersonic vehicles; thermal environment; film cooling; CFD

1. Background

Severe aerodynamic surface heating is one of the major problems in the development of reusable launch vehicles traveling at hypersonic Mach numbers. Current state of art of thermal protection system lacks capability when facing this situation and could increase the weight of the vehicle to some degree, or increase the complexity of the aerospace surface. On the other hand, film cooling has been widely used as an effective way of active cooling in the application of turbine engines for aeroplane[1]. The number of papers on film cooling has reached as many as nearly ten thousands. Currently there are a few researches on film cooling for hypersonic vehicles， but the speed limit is no higher than 10 Ma[2][3][4]; the inject hole is not located at the stagnation area[5][6]; the shape of the inject hole is simply cylinder[7], which is less efficient than shaped hole.

The active thermal protection technic called film cooling for hypersonic vehicles over Mach 20 was presented here; via numerical methods (computational fluid dynamics, CFD), the cooling efficiency of film cooling was calculated, and the feasibility of film cooling for hypersonic vehicles was validated through test.

2. Theories

2.1 Governing equations for hypersonic viscous flow

For a chemically reacting flow, the complete Navier-Stokes equations are [8]:

$$\frac{\partial Q}{\partial t}+\frac{\partial E}{\partial x}+\frac{\partial F}{\partial y}+\frac{\partial G}{\partial z}=\frac{\partial E_v}{\partial x}+\frac{\partial F_v}{\partial y}+\frac{\partial G_v}{\partial z}+S. \tag{1}$$

In which Q is the state vector of conservative variables, E , F , G are convective flux vectors, E_v , F_v , G_v are viscous flux vectors, S is the chemical source term, and these variables and vectors can be expressed as follows:

$$Q=\begin{bmatrix}\rho_s\\ \rho u\\ \rho v\\ \rho w\\ E_t\end{bmatrix},E=\begin{bmatrix}\rho_s u\\ \rho u^2+p\\ \rho uv\\ \rho uw\\ (E_t+p)u\end{bmatrix},S=\begin{bmatrix}\dot{\omega}_s\\ 0\\ 0\\ 0\\ 0\end{bmatrix},E_v=\begin{bmatrix}-\rho_s u_s\\ \tau_{xx}\\ \tau_{xy}\\ \tau_{xz}\\ (u\tau_{xx}+v\tau_{xy}+w\tau_{xz}+\kappa\dfrac{\partial T}{\partial x}+\sum_{s=1}^{ns}h_s\rho_s U_s\end{bmatrix}. \quad (2)$$

Where, F_v , G_v have the similar form as E_v . Here, ρ_s , U_s , h_s represent the density, diffusion speed and enthalpy of species s; E_t is the total energy of gas mixture per unit volume; $\dot{\omega}_s$ is the net mass rate of production of species per unit volume; τ_{xx} , τ_{xy} , etc., are stress tensors.

2.2 Chemically Reaction Scheme

2.2.1 Chemical reaction equation

For reaction flows, a general finite rate reaction equation may be written as:

$$\sum_{i=1}^{n}\nu'_{ik}M_i \leftrightarrow \sum_{i=1}^{n}\nu''_{ik}M_i, \qquad k=1,2,...,K. \quad (3)$$

Where ν'_{ik} and ν''_{ik} are stoichiometric coefficients for the reaction and M_i represents an arbitrary molecule in the reaction.

2.2.2 Chemical reaction rates

The forward rate at which chemical reactions proceeded was calculated using a modified Arrhenius relation whilst the backwards rate was modelled by assuming equilibrium:

$$K_f=C_1T^{\eta}e^{[\frac{-\varepsilon_0}{kT}]},\ K_b=\frac{K_f}{K_{eq}} \quad (4)$$

C_1, η and $\frac{-\varepsilon_0}{k}$ are experimentally derived constants which differ for each reaction. The reaction scheme also contained a third body (M) for each of the dissociation reactions and a corresponding third body efficiency (eff_M).The reaction scheme used in this study is PARK-I[9], which is one of the most common schemes used for modelling the chemistry of air without the consideration of ionization. The PARK-I reaction scheme involves 5 species (N_2、O_2、N、O and NO) and seventeen reactions. These reactions and their corresponding rate data (SI units) are listed in Table 1.

Table 1: Park-1 reaction scheme for air

Reaction type	Reaction function	Third body M	Frequency Factor C_1	Third body efficiency $\mathrm{eff_M}$	Temprature factor η	Reaction energy $\frac{-\varepsilon_0}{k}$
Dissociation	$O_2+M\leftrightarrow 2O+M$	N	8.25×10^{16}	3.0	-1.00	59500
		N_2	2.75×10^{16}	1.0	-1.00	59500
		O	8.25×10^{16}	3.0	-1.00	59500
		O_2	2.75×10^{16}	1.0	-1.00	59500
		NO	2.75×10^{16}	1.0	-1.00	59500

Dissociation	$N_2 + M \leftrightarrow 2N + M$	N	1.11×10^{19}	3.0	-1.60	113200
		N_2	3.70×10^{18}	1.0	-1.60	113200
		O	1.11×10^{19}	3.0	-1.60	113200
		O_2	3.70×10^{18}	1.0	-1.60	113200
		NO	3.70×10^{18}	1.0	-1.60	113200
Dissociation	$NO + M \leftrightarrow N + O + M$	N	4.60×10^{14}	2.0	-0.50	77500
		N_2	2.30×10^{14}	1.0	-0.50	77500
		O	4.60×10^{14}	2.0	-0.50	77500
		O_2	2.30×10^{14}	1.0	-0.50	77500
		NO	2.30×10^{14}	1.0	-0.50	77500
Neutral exchange	$NO + O \leftrightarrow N + O_2$	-	2.16×10^{5}	-	1.29	19220
Neutral exchange	$O + N_2 \leftrightarrow N + NO$	-	3.18×10^{10}	-	0.10	37700

3. Validation of CFD code

In order to validate our CFD code, we modelled and calculated the experiments from NASA TN D-5450[10].

3.1 Geometry model

The geometry model is shown in Fig. 1, in which $\theta_C = 15°$. The freestream speed is V=1461.92 m/s, temperature condition is: $T_\infty = 47.34\ K$, the wall is isothermal (300K). We chose 4 typical cases from experimental results. In case 1 and 2, the radius of the head of the cone is 0.008525 m, the pressure of the free flow is 132.06 Pa, while for case 3 and 4, the radius of the head of the cone is 0.02794m, and the pressure of the free flow is 198.09 Pa. In case 1 and 3, the angle of attack is 0 degree, while in case 2 and 4, the angle of attack is 20 degree.

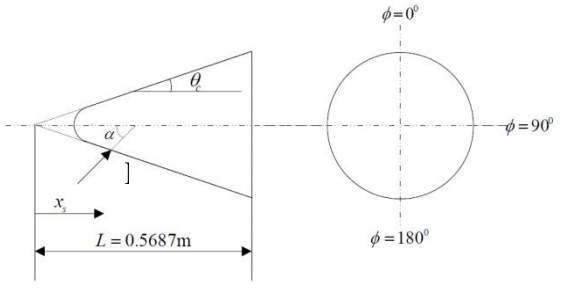

Figure 1: Geometry of validation model-cone

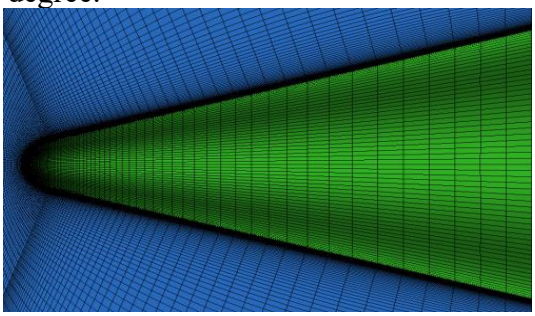

Figure 2: Grid of the model

Half of the model is built to save computation resource. Structured grid is built using ICEM, the grid is clustered and refined in the vicinity of wall, with the height of the first layer of the grid in the normal wall direction being 0.001mm. The number of grid is 702108 for case 1 and 2 and 458370 for case 3 and 4, shown in Fig. 2. Due to the experiment condition, the laminar flow model was used, with the flux splitting scheme using Van Leer's FVS scheme, with flux limiter using Osher-C (L).

3.2 Results

The CFD results are compared with experimental results in Fig. 3. The calculation matches well with experimental results; under certain conditions, such that in case 2 and 4 (angle of attack is not zero), the CFD results for windward side is a little bit too low. This is probably because when the angle of attack is not zero, the flow separates from the windward side of the wall, and the laminar model underestimated the heat flux.

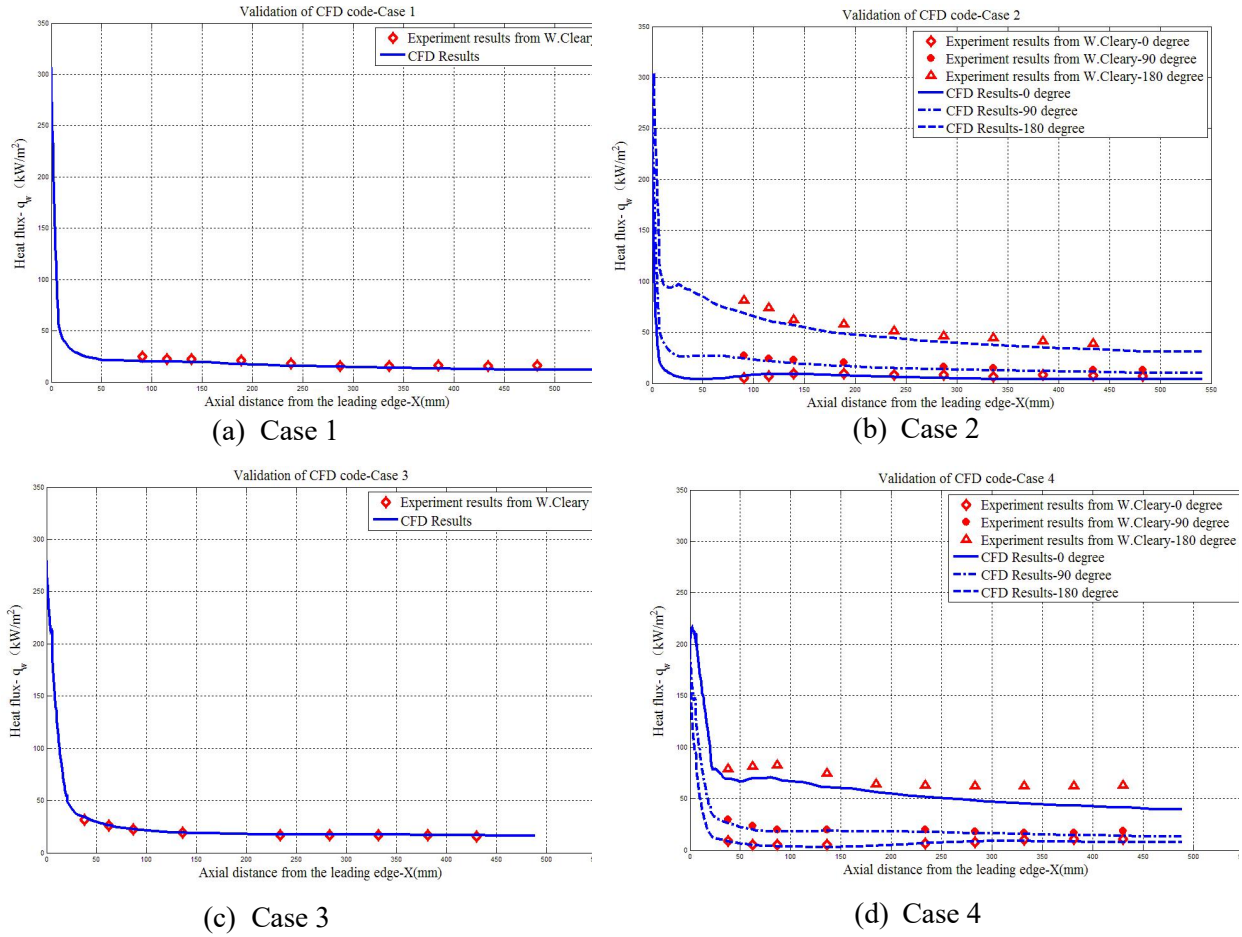

Figure 3: Comparison of CFD results with experimental data

4. Cone film cooling active thermal protection simulation

The effectiveness of film cooling for hypersonic vehicles was studied via numerical simulation in this section.

4.1 Model setup

The cone model was used again. First, the model without film cooling was built for comparison. Then the model with several special designed shaped film cooling holes located around the stagnation region of the cone was built. One central expanding hole with a diameter of 0.5mm was located at the stagnation region, and 13 shaped holes with a diameter of 0.5mm were distributed radially uniformly. The angle between the shaped hole axis and central hole axis was 12 degree. The grid was refined in the vicinity of wall and the hole to capture the flow feature. The height of the first layer of the grid in the normal direction was 0.01mm. The grid was optimized by trial and error to balance the accuracy and the computation resource. The final model was shown in Fig. 4 and Fig. 5, and only half of the model was calculated considering the symmetry.

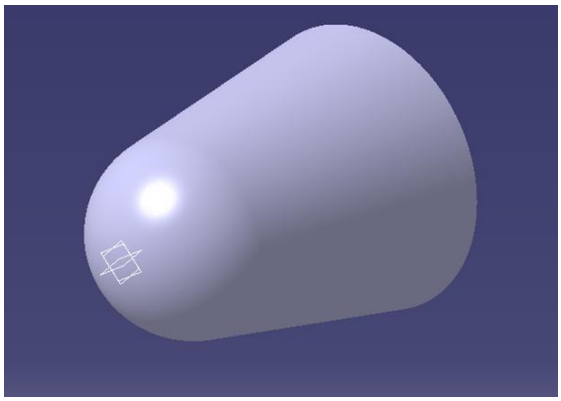

Figure 4: CAD model without film cooling holes

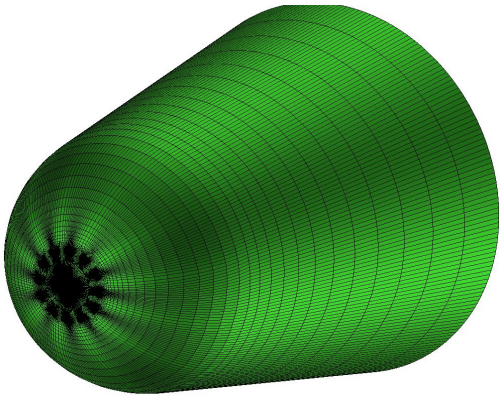

Figure 5: Grid model with film cooling holes

Typical free stream condition was chosen as the height of 50 km and speed of 15 Ma. The pressure is $P_\infty = 87.86\,\mathrm{Pa}$, the temperature is $T_\infty = 282.7\,\mathrm{K}$. Velocity inlet boundary condition was used, with a static pressure of 0.5MPa at the inlet for coolant gas, the static temperature was 100K and the inlet velocity was 200 m/s, meanwhile keeping the total pressure and total temperature at constant number. Radiation thermal equilibrium condition was used at the wall and the thermal radiation coefficient was 0.95. Turbulence was modelled with Menter's two-equation shear stress transport (SST) k-ω model[11]. The SST model uses the k-ω formulation close to the wall, blending to the k-ε model toward the free stream. This model is less sensitive to specification of free stream turbulence level compared to the k-ω model and performs comparatively well in adverse pressure gradients and separated flows. All calculations are set up using the 5 species, 17 reaction scheme of PARK-I.

4.2 Simulation results

4.2.1 Model without film cooling

Fig. 6 and Fig. 7 show the temperature and heat flux distribution contour of the model without film cooling. The temperature at the stagnation point could reach 3430 K, and the heat flux at the stagnation point is 7879kW/m^2.

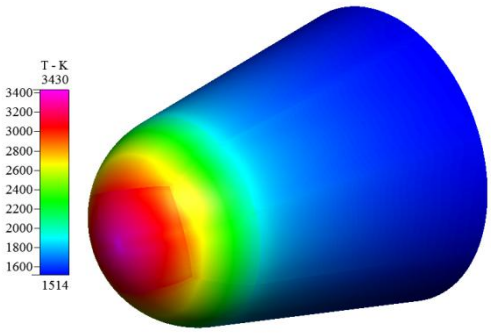

Figure 6: Contour of temperature (no film cooling)

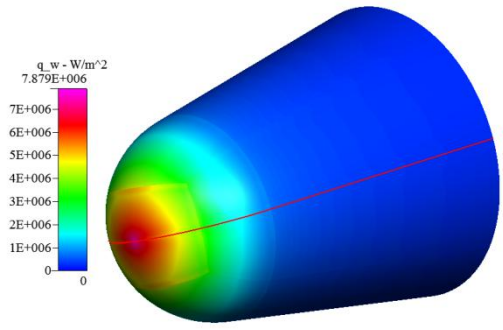

Figure 7: Contour of heat flux (no film cooling)

4.2.2 Model with film cooling

Fig. 8 and Fig. 9 show the temperature and heat flux distribution contour of the model with film cooling. The peak temperature at the wall is reduced to 2131K, and the heat flux is reduced to 1111kW/ m^2.

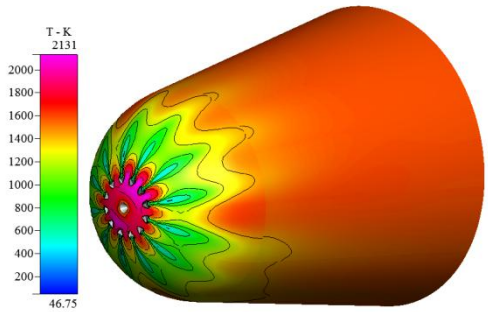

Figure 8: Contour of temperature (film cooling)

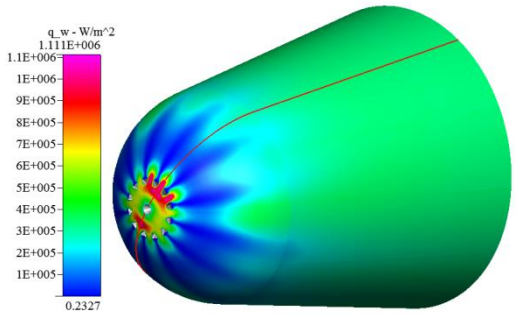

Figure 9: Contour of heat flux (film cooling)

The temperature contour of the symmetry plane is shown in Fig. 10. The simulation shows that the structure of shock waves is complicated. There is a Mach disk in front of the jet outlet. After passing through the Mach disk, the opposing jet interacts with the free stream and forms a thin bow shock. Due to the jet flow, the bow shock twists and is pushed away from the head of the cone. Jet flow recirculates and reattaches the wall pushed by the free stream, forming a recirculation region near the hole. Due to the mixture of free stream with the jet flow, the peak temperature of air at the wall is greatly reduced. The flow field characteristics include shock wave, Mach disk, shear layer, recirculation zone, shock-shock interference, shock-boundary layer interference. The CFD result successfully catches the complex flow structure induced by the interaction of the coolant jet and the shock wave.

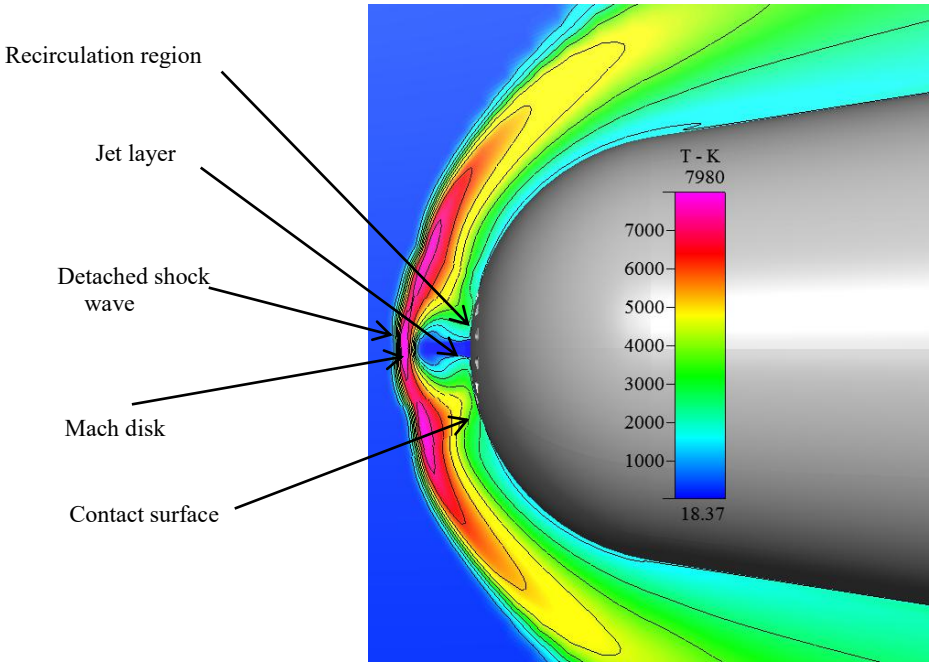

Figure 10: Contour of temperature with film cooling

Fig. 11 shows the vector plot of velocity near the hole and from which the flow direction of flow can be seen clearly. After interaction with the free stream, the jet flow forms clockwise vortex structure and flows to the downstream along the wall, and that means the multi-hole jet flow design is effective.

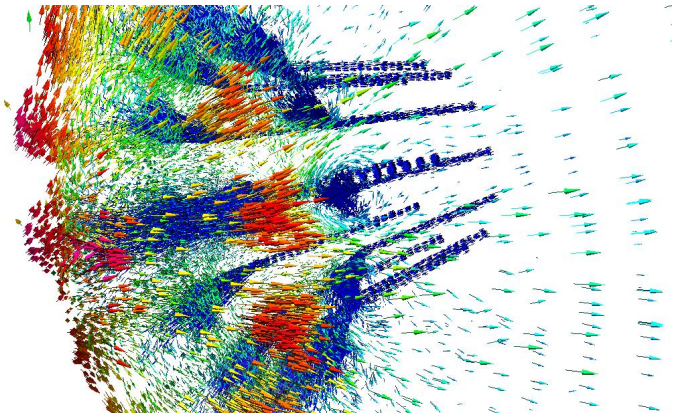

Figure 11: Vector plot of the flow

5. Test validation

In the first test, a cone with shaped hole was put in a vacuum chamber with a pressure under 10Pa. 4 thermocouples were located at different positions on the cone, the first one was put at the intersection between the spherical surface and the cone, and the other three were uniform-spaced along the cone element. Firstly, the cone was heated through plasma and naturally temperature at different positons rose rapidly (shown in Fig. 12 and Fig. 13). Then low temperature nitrogen gas with a pressure of 0.05 MPa supplied by Liquid nitrogen tank jetted from the shaped hole, test results showed that temperature at different positons fell rapidly(shown in Fig. 14 and Fig. 15).

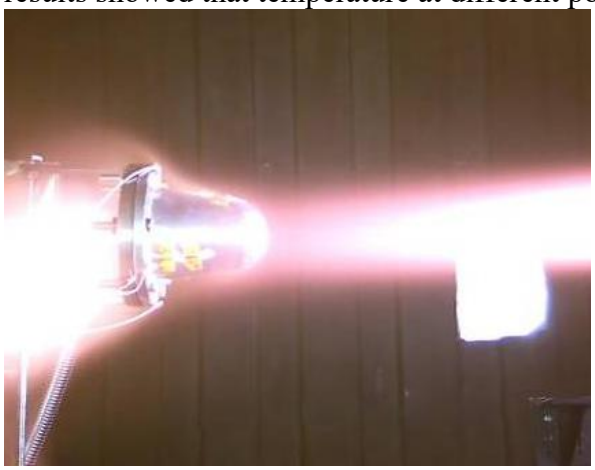

Figure 12: Cone heated by plasma (no cooling)

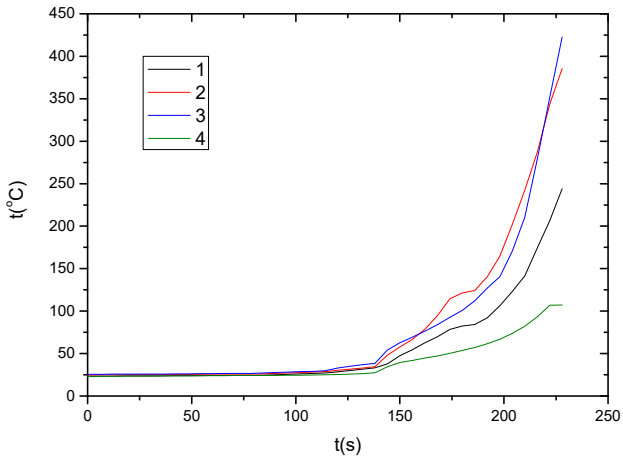

Figure 13: Temperature on the cone (no cooling)

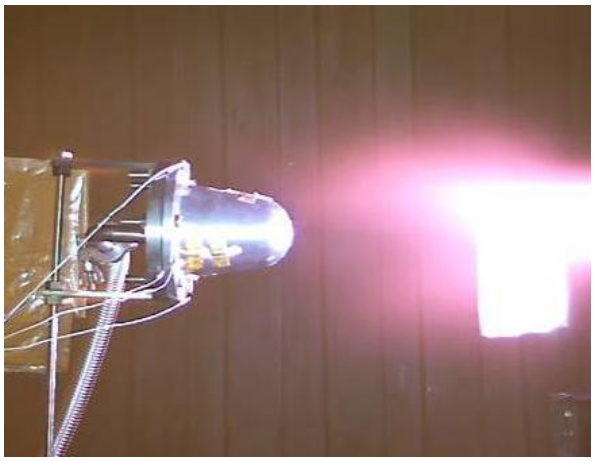

Figure 14: Cone heated by plasma (with cooling)

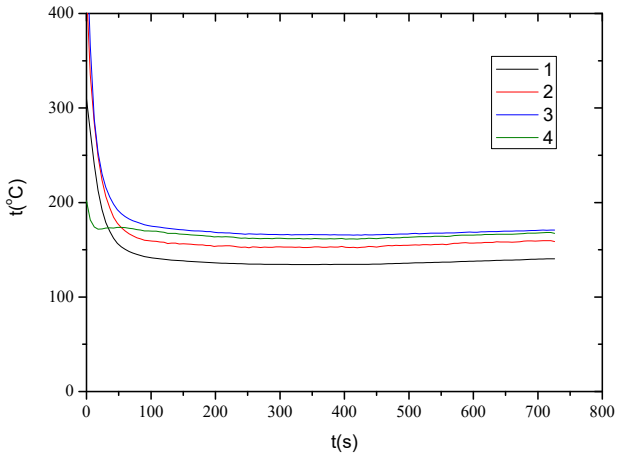

Figure 15: Temperature on the cone (with cooling)

Test through heat source with a welding gun had also shown similar effect, as shown in Fig 16.

Figure 16: Cone heated by welding gun (with active cooling)

6. Conclusion

A new approach of thermal protection system for hypersonic vehicle is presented. Research has been focused on the cooling effectiveness of multi-hole jet flow. The result showed promising performance of film cooling for hypersonic vehicles.

REFERENCES

[1] Ronald S. Bunker, A Review of Shaped Hole Turbine Film-Cooling Technology, Journal of Heat Transfer, APRIL 2005, Vol. 127/ 441, DOI:10.1115/1.1860562.

[2] Adrian S. Pudsey, Russell R. Boyce, and Vincent Wheatley, Hypersonic Viscous Drag Reduction via Multiporthole Injector Arrays, Journal of Propulsion and Power, Vol. 29, No. 5, 2013.

[3] K.A. Heufer and H. Olivier, Film Cooling of an Inclined Flat Plate in Hypersonic Flow, 14th AIAA/AHI Space Planes and Hypersonic Systems and Technologies Conference, AIAA 2006-8067.

[4] K. A. Heufer and H. Olivier, Experimental and Numerical Study of Cooling Gas Injection in Laminar Supersonic Flow, AIAA JOURNAL, Vol. 46, No. 11, November 2008.

[5] Sung In Kim and Ibrahim Hassan, Numerical Study of Film Cooling Scheme On A Blunt-Nosed Body In Hypersonic Flow, Proceedings of the ASME 2010 International Mechanical Engineering Congress & Exposition, IMECE2010, November 12-18, 2010, Vancouver, British Columbia, Canada, IMECE2010-40496.

[6] Sung In Kim and Ibrahim Hassan, Numerical Study of Film Cooling Scheme on a Blunt-Nosed Body in Hypersonic Flow, Journal of Thermal Science and Engineering Applications, DECEMBER 2011, Vol. 3 / 044501-1.

[7] Jeswin Joseph and S.R. Shine, Coolant Gas Injection On A Blunt-Nosed Re-Entry Vehicle, Proceedings of the ASME 2013 Gas Turbine India Conference GTINDIA2013 December 5-6, 2013, Bangalore, Karnataka, India.

[8] John D. Anderson, Jr., Hypersonic and High-Temperature Gas Dynamics, AIAA education series.

[9] Park, C., On Convergence of Computation of Chemically Reacting Flows, AIAA,(85-0247), 1985. 23rd AIAA Aerospace Sciences Meeting, January 14-17,1985.

[10] Joseph W. Cleary, Effects Of Angle Of Attack and Bluntness on Laminar Heating-Rate Distributions of A 15° Cone At A Mach Number Of 10.6, Ames Research Center, NASA TN D-5450,1969.

[11] Menter, F. R., Two-Equation Eddy-Viscosity Turbulence Models for Engineering Applications, AIAA Journal, Vol. 32, No. 8, 1994, pp. 1598–1605. doi:10.2514/3.12149.